https://doi.org/10.48048/tis.2022.3092

Effects on Structural Morphological and Optical Properties Pure and CuO/ZnO Nanocomposite

Pradip Sable, Nabeel Thabet, Jameel Yaseen and Gopichand Dharne*

Department of Physics, Dr. Babasaheb Ambedkar Marathwada University, Maharashtra, India

(*Corresponding author's e-mail: drgmdharne@gmail.com)

Received: 7 March 2022, Revised: 23 April 2022, Accepted: 30 April 2022, Published: 19 November 2022

Abstract

In the present work, synthesis of CuO, ZnO and CuO/ZnO Nonocomposites and their properties have been investigated. CuO, ZnO and CuO/ZnO NC were synthesized using the co-precipitation method. The nanocomposite materials were structural, morphological and optical properties characterized by X-ray diffraction (XRD), Field Emission Scanning Electron microscopy (FESEM), energy-dispersive X-ray spectroscopy (EDX), Fourier transform infrared spectroscopy (FTIR), UV-Vis Spectroscopy. The results of the XRD analysis exhibited that the pure CuO, ZnO and CuO/ZnO NC has a nanometer size with an average of 15.19 nm. The UV-vis analysis showed that the CuO, ZnO and CuO/ZnO NC has a band-gap of 3.31 and 2.35 eV. FTIR investigation revealed that the vibration of ZnO was observed at 561 cm^{-1} whereas CuO was at 602 cm^{-1} and composites 612 cm^{-1}. The FESEM-EDX analysis revealed that the ZnO has a hexagonal structure whereas the CuO has a monoclinic structure.

Keywords: XRD, FESEM-EDX, FTIR, UV-Vis, CuO, ZnO, CuO/ZnO Composites

Introduction

A nanomaterial is a material with a size range of 1 to 100 nm. Nanoparticles have a small particle size, a narrow pore size distribution, little agglomeration, and high dispersion [1-5]. Gas sensors, beauty products, medicine, displays, batteries, paints, catalysis, food engineering (manufacturing, processing, safety, and packaging), farming, energy (storage and conversion), and construction are just a few of the applications for nanomaterial's [6-12]. In recent years, various forms, shapes, and sizes of photo catalytic activities for the removal of dye impurities have been identified [13]. The scientific community has become more interested in recent efforts to produce semiconductor oxide materials. Due to its electrical and optical properties, cupric oxide (CuO) is a commonly utilized semiconductor. This oxide is a p-type semiconductor with a band gap of 1.2 eV [14-16]. Zinc oxide is an inorganic compound that is found only in small amounts in nature. Zinc oxide exhibits semiconductor and piezoelectric capabilities due to its huge 3.37 eV bandgap and high 60 meV binding energy [17,18]. Recently, different forms of metal oxide nanocomposites, synthesized such as ZnO/Mg, CuO/ZnO, ZnO/NiO, Co_3O_4/ZnO, and CeO_2/ZnO, have been recently produced [19-21]. Nanocomposites materials are made up of many phases, at least one of which has a nanoscale structure that gives the nanocomposites its size-dependent properties. Nanocomposites have the potential to combine the desirable qualities of various nanoscale building blocks, allowing for the tailoring of material properties for device fabrication for specific applications [22]. Hassanzadeh *et al.* [23] remove methyl orange dye from aqueous solutions, a ZnO/CuO nanocomposite immobilized γ-Al_2O_3 was prepared via a heterogeneous precipitation method. Abraham *et al.* [24] through optimum integration with sensing layers, SAW-based sensor technology is particularly promising for sensing any analyte. In COMSOL Multiphysics, SAW gas sensors based on CNT and ZnO-CuO/CNT nanocomposites were modeled. Their reaction to various VOCs has been studied at room temperature. Das and Srivastava [25], the synthesis of ZnO/CuO nanocomposite by electrochemical technique is described for the first time in this communication. The anode was made up of zinc and copper electrodes, with aqueous succinic acid as the cathode. The solution was utilized as an electrolyte to make ZnO/CuO nanocomposite, which was then analysed using advanced techniques. Using a 3-electrode cell setup, the electrochemical performance of nanocomposite was investigated in bare sodium hydroxide solution. It has a monoclinic crystal structure as well as. The co-precipitation method process is used to make CuO, ZnO and CuO/ZnO nanocomposites in varied quantities. X-ray diffraction (XRD), Field Emission scanning electron microscopy (FESEM), energy-dispersive X-ray spectroscopy (EDX), and Fourier transform infrared spectroscopy (FTIR) are used to characterize the produced composites

(FTIR) also UV-Vis spectroscopy. The features of the increased CuO and ZnO composites performance are also reviewed in terms of applications.

Materials and methods

Chemical and reagents

Zinc(II) acetate dehydrate ($Zn(CH_3COO)_2.2H_2O$) 98 %, copper(II) sulphate pentahydrate ($CuSO_4.5H_2O$) 98 %, ethanol, NaOH, and distilled water. All chemicals provided were analytical reagent (AR) grade and were utilized without additional purification. Zinc acetate, Copper sulphate, sodium hydroxide were acquired from Fisher Scientific chemicals in Mumbai.

Synthesis of CuO, ZnO and CuO/ZnO nanocomposites

Synthesis of nanoparticles used the co-precipitation method. Typically, 0.1 M of Zinc acetate $Zn(CH_3COO)_2.2H_2O$ was dissolved in 80 mL double distilled water also 0.1 M copper sulphate ($CuSO4.5H_2O$) was dissolved in 80 mL DDW. Composites taking different molarity copper sulphate and Zinc acetate (0.05 M, 0.05 M) and stirred with a magnetic stirrer for an hour. Precipitation was obtained that precipitation was filtered by Whatman filter paper. The precipitation was washed several times with distilled and dry 2 days this typical experiment was carried out. The complete experiment was carried out at 60 °C temperature with optimized. Same process followed by CuO and CuO/ZnO NC. The different nanoparticles were prepared respectively. The prepared material grinds in mortal pestle at the time powder form. As-prepared nanoparticles were annealed in muffled furnace at 500 °C for 3 h and used for further characterizations. These materials were characterized by X-ray diffraction (XRD), Field emission scanning electron microscopy (FESEM), Fourier transform infrared spectroscopy (FTIR), Energy dispersive x-ray analysis (EDX) and UV-vis-spectroscopy.

Results and discussion

X-ray diffraction

X-ray diffraction was used to confirm the nanomaterial's crystal structures. The XRD patterns of CuO, ZnO and CuO/ZnO nanocomposites with varying copper concentrations are shown in the **Figure 1**. The peaks at these 2θ values correspond to the crystal planes of 110, 002, 101, 102, 110, 103, 200, 112, 021, 201, 004, and 202 in CuO (50 %) ZnO (50 %) NC. The nanocomposite 2θ value indices were found to be 31, 34, 35, 36, 38, 47, 48, 56, 58, 61, 62, 66, and 68 degrees, respectively [26]. Major peaks were found at roughly 31.82 (100), 34.50 (002), and 36.32 (101) of the undoped ZnO, as indicated by the bar in the Miller indices. A small peak at 38.8 was observed in CuO/ZnO nanocomposites, which was indexed to CuO (111). The diffraction intensities and angles altered dramatically when Cu was added to ZnO [27,28]. CuO (111) diffraction peaks were discovered with copper contents. Furthermore, as copper concentrations increased, no other peaks or significant shifts were observed, and no solid solution formed between CuO and ZnO. The grain size of the ZnO and CuO/ZnO nanocomposites was calculated using the Scherrer equation. $D = K\lambda/\beta\cos\theta$ where, K-scherrer constant, λ-wavelength of radiation, β-full width half maximum, θ-Braggs angle [29]. The estimated average grains size was 15.19 nm for ZnO, CuO and CuO/ZnO NC, respectively. For the average crystallite size was measured as 21, 19 and 15.19 nm. The average particle size was found to be 15.19 nm, indicating that the particle size was larger than the typical crystallite size. The crystallinity of the samples was also clearly revealed by XRD data. Different types of intensity [30].

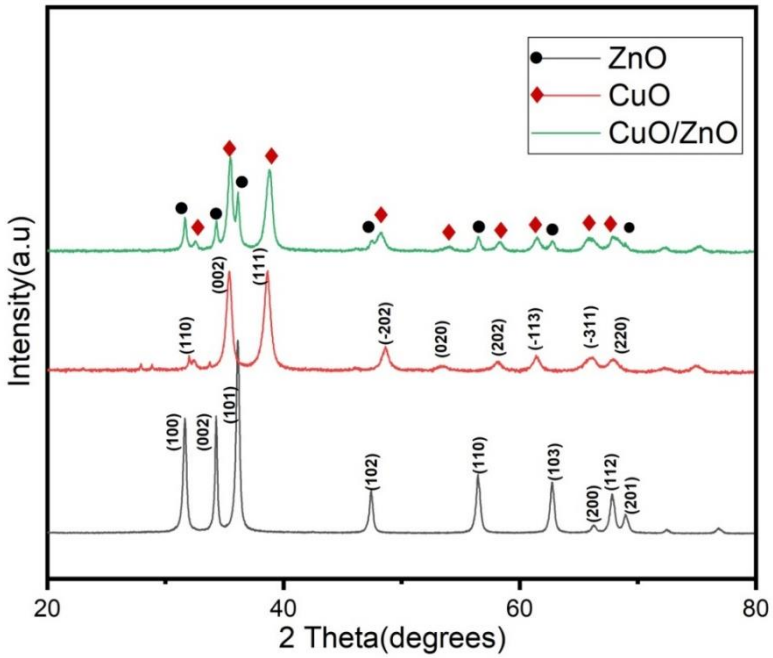

Figure 1 X-ray diffraction (XRD) patterns of CuO, ZnO and CuO/ZnO.

FESEM and EDX study

The particle sizes and surface morphology of CuO/ZnO NC unground composite powders were investigated using FESEM analysis. Particles of various sizes are created as a result of this process Aggregated. Due to the high heat produced by the combustion reaction and the calcination process, particles are visible in the FESEM analysis images. The FESEM micrographs of pure ZnO powder in **Figure 2(a)** and **2(b)** indicate their different sizes in flower form, ranging from 2 µm to 200 nm. The FESEM micrographs (a and d) show pure CuO powders with a roughly hexagonal shape and average particle sizes of around 1 µ and 200 nm [31,32]. The clarity and chemical content of the produced samples were investigated using energy dispersive spectroscopy. The EDX spectrum, as shown in **Figure 3** contains just elemental copper (Cu) and oxide (O), also zinc (Zn) and oxide (O) with no additional elemental impurities detected. EDX examination validated its purity phase of the CuO-ZnO NC Fig. Cu = 57.26, Zn = 5.27, O = 37.47 was found, which was consistent with the hypothesis. The elements ratio exact stoichiometry was employed for preparing. The development of pure CuO-ZnO was revealed by the elimination of any impurities. Nanoparticles, which back up the findings of the study XRD information [33,34]. The CuO/ZnO alloys show a considerable morphological change. When such 2 oxides are appropriately proportioned, as in the percent sample, more uniform nanoparticles are formed, providing regular distribution and consistency. When the CuO concentration is greater, such as 50 % ZnO and 50 % CuO, the samples take on a variety of morphologies, including hexagonal structures and complex shapes. The grain sizes are distributed in the 200 nm range. It's also worthy of note that the pores that appear in CuO/ZnO Nanoparticle are the product of CuO/ZnO crystal aggregates. When powders are utilised as catalysts, the structural shape of associated pores [35].

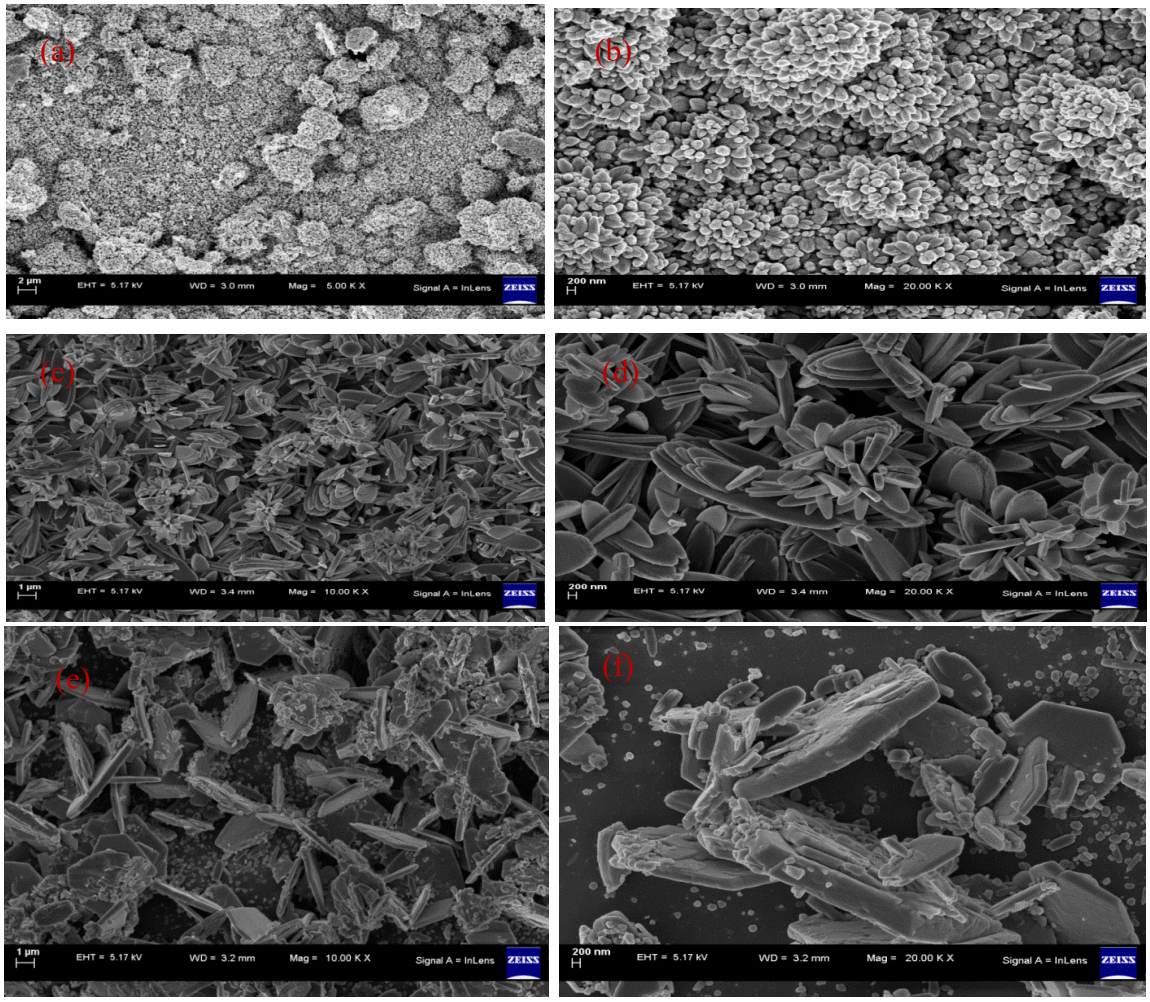

Figure 2 FESEM of ZnO (a and b) CuO (c and d) and Nanocomposites CuO/ZnO (e and f).

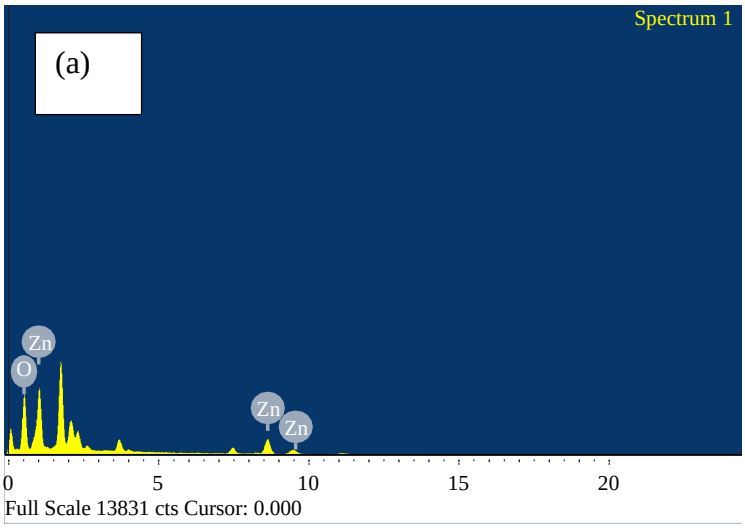

Element	Weight%	Atomic%
O	57.22	84.53
Zn	42.78	15.47
Totals	100	

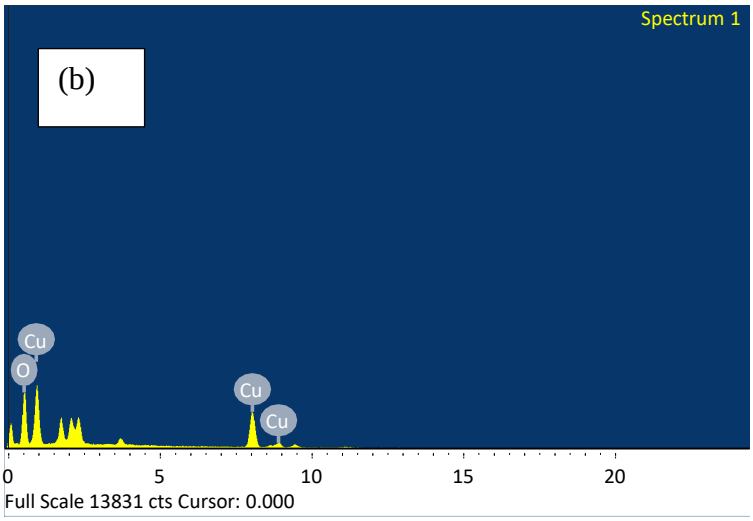

Element	Weight%	Atomic%
O	41.24	73.60
Cu	58.76	26.40
Totals	100	

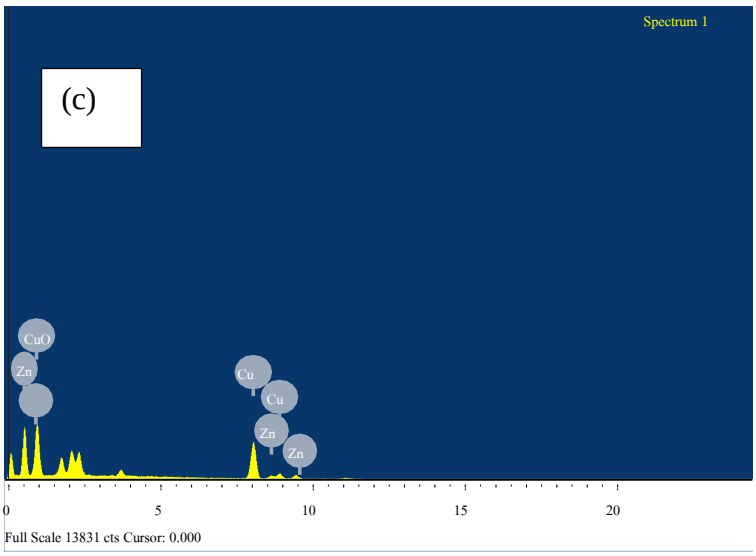

Element	Weight%	Atomic%
O	37.47	70.46
Cu	57.26	27.11
Zn	5.27	2.43
Totals	100	

Figure 3 EDX spectrum pure ZnO (a), CuO (b), and CuO/ZnO (c) nanocomposites.

FTIR Spectrophotometer

FTIR spectrophotometer was used to analyze the functional group of CuO, ZnO and CuO/ZnO Nanocomposites. The wavelength of 4000 - 500 cm^{-1} was used. For the analysis of functional groups of samples and the results can be seen in **Figure 4**. FTIR spectra of CuO, ZnO and CuO/ZnO nanoparticles are presented in **Figure 4**. The spectra show optical phonon modes centered at 561 and 524 cm^{-1} for CuO, ZnO and CuO/ZnO nanocomposites, respectively [36]. The FTIR modes depend on the size, shape, and state of aggregation of the nanoparticles. From the FESEM analysis, it is inferred that only ZnO nanoparticles are present in ZnO system while in CuO/ZnO system, both CuO and ZnO nanoparticles are present, which differ in size, shape, and aggregation. This is the reason why the 2 systems show modes at different wavenumbers. In CuO/ZnO, the contribution also comes from the vibrational mode of CuO, which is around 602 cm^{-1}. The modes at higher wavenumbers are associated with the vibrational modes of various impurities such as hydroxylate, carboxylate, and alkane in the materials. In ZnO, the modes are not distinct and there are more noises. For CuO/ZnO nanoparticles, the peak at 1378, 1383, 1420 cm^{-1} is assigned to the symmetric stretching of the carboxyl group, C=O. The transmittance peak at 2315 cm^{-1} is associated with the CO2 molecule in air. The broad peak at around 3738 cm^{-1} and the peak at 1511 cm^{-1} have their origin from the stretching vibration of O=H groups. The OH peak at around 2986 cm^{-1} is associated with different defects and increased free-carrier concentration [37,38].

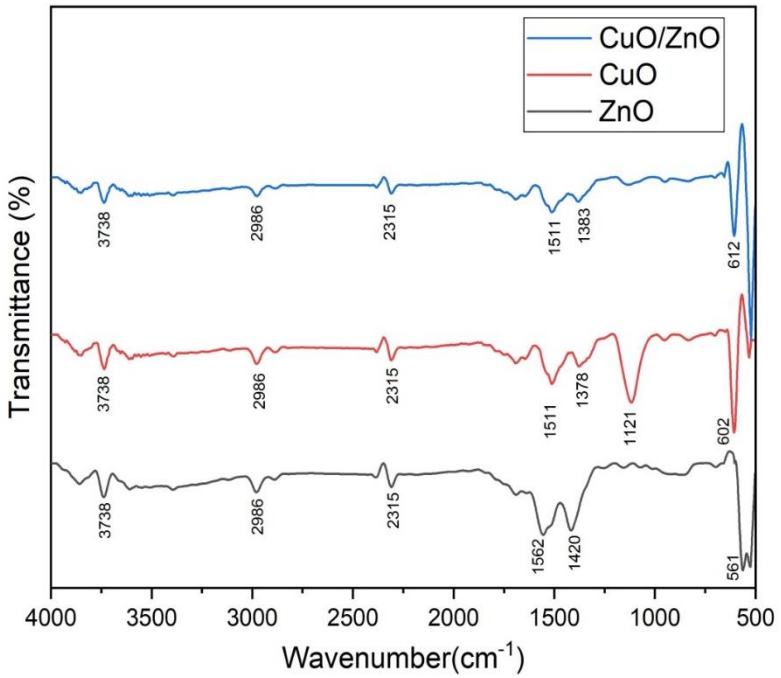

Figure 4 FTIR spectra of ZnO, CuO, and CuO/ZnO nanocomposite.

UV-Vis. spectroscopy

The UV-Vis absorption spectra of CuO, ZnO, nanoparticles and hybrid CuO/ZnO NC are shown in **Figures 5** with a CuO, ZnO and CuO/ZnO NC inset. CuO, ZnO nanoparticles, and CuO/ZnO NC have unique absorption peaks positioned at 295, 298 and 296 nm, respectively [39,40]. The absorption peaks of CuO, ZnO nanoparticles are extremely similar to those reported in prior literature. The addition of ZnO, CuO nanoparticles resulted in a large red shift in the absorption spectra, whereas the CuO absorption peak vanished completely, possibly due to the formation of core-shell structured CuO/ZnO NC. CuO, ZnO and CuO/ZnO NC have energy gaps of the values observed for the composites materials CuO/ZnO (50:50) shows 2 different band gap absorption energy levels 2.97 - 3.27 and 2.35 - 3.31 eV, respectively, as calculated from absorption spectra [41-43]. The combination CuO/ZnO NC reduced energy gap and near-visible region absorption imply that it could be a promising material for visible light. The optical behavior of the materials was investigated using UV-visible spectroscopy over the wavelength range of 200 - 700 nm. The sample's energy gap (Eg) was calculated using Tauc's equation $(\alpha h\upsilon)2 = A(\alpha h\upsilon\text{-}Eg)n$, where h, A, and Eg are the absorption coefficients as shown **Figures 6** [44].

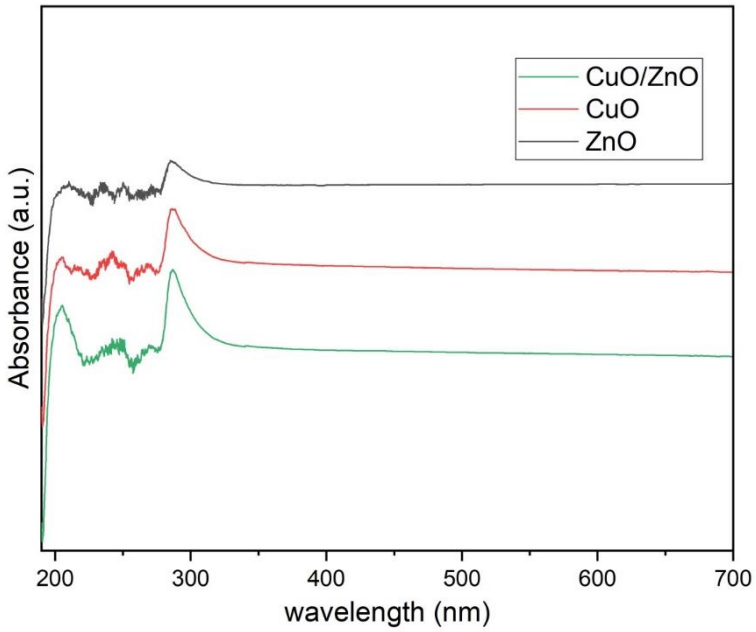

Figure 5 Optical absorbance spectra of pure ZnO, CuO and CuO/ZnO composite.

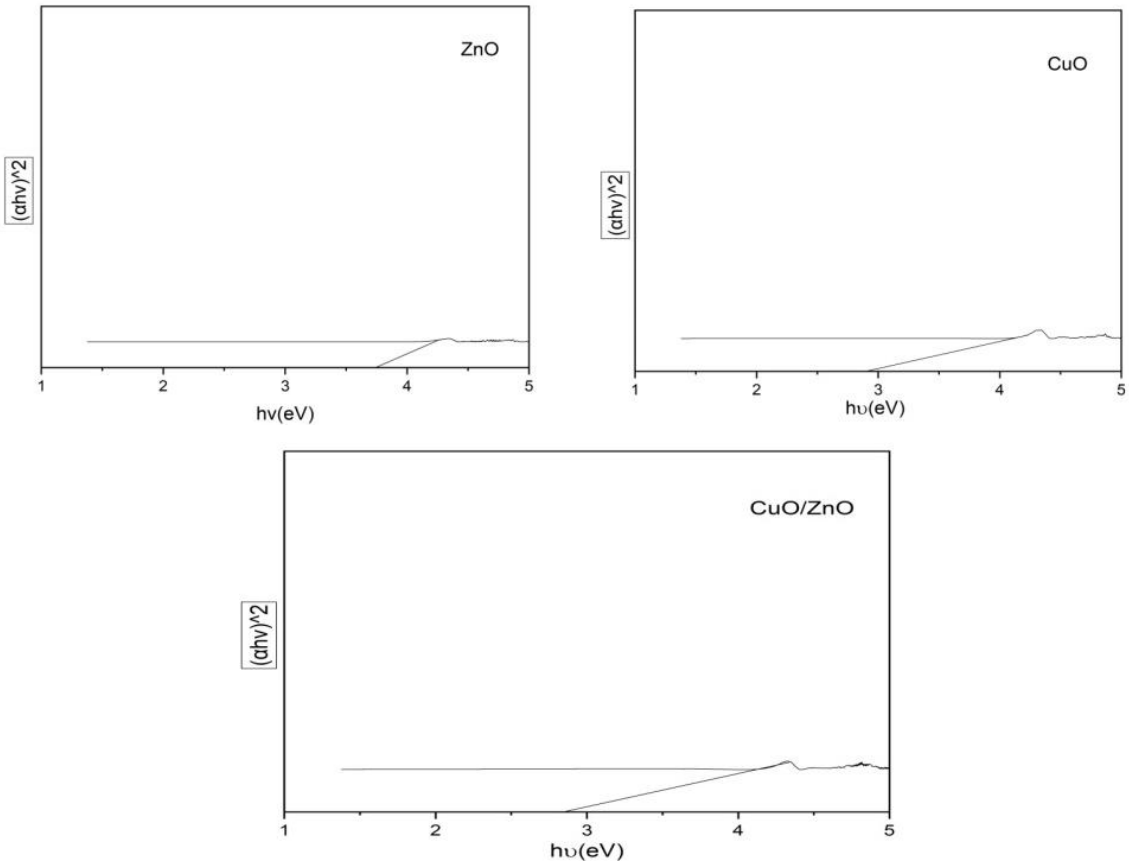

Figure 6 Tauc plot pure and composites.

Conclusions

The CuO, ZnO and CuO/ZnO nonocomposites were successfully synthesized using co-precipitation method. For the average crystallite size was measured as 21, 19, and 15.19 nm, observed in composite for the CuO content of 50 %, and ZnO 50 %, respectively. Addition of CuO reduced the value of the band gap energy of ZnO i.e. 3.31, 2.35 eV, CuO/ZnO (50:50) shows 2.97 - 3.27 eV. The nanocomposites were grown and uniformly, while the CuO nanostructures with a thickness of were grown epitaxially on to the ZnO nanostructured, according to morphological and structural analysis. The optical property analysis showed that the prepared fundamental nanocomposite nanostructured acquired developed light absorption ability in the visible region. The obtained CuO/ZnO nanocomposites were optimized and characterized by XRD, FESEM, and FTIR to obtain their chemical and morphological and optical properties. The findings of this study have contributed to advanced device nanostructures, which are the foundation of functional nanodevices for the development of new nanostructured phases and are favorable for their applications.

Acknowledgements

The authors are grateful to Dr. Babasaheb Ambedkar Marathwada University, Aurangabad, Department of Physics, RUSA center for XRD, UV, and Labzone Services Provide Consultancy, data interpretation and material testing services Mumbai India for FESEM, EDX, also archaeological survey of India, Dr. Babasaheb Ambedkar Marathwada University, Aurangabad, for FTIR characterization.

References

[1] JH Huang, JX Chen, YF Tu, Y Tian, D Zhou, G Zheng, JP Sang and QM Fu. Preparation and photocatalytic activity of CuO/ZnO composite nanostructured films. *Mater. Res. Express* 2018; **6**, 015035.

[2] MG Lines. Nanomaterials for practical functional uses *J. Alloys Comp.* 2008; **449**, 242-5.

[3] H Amrulloh, YS Kurniawan, C Ichsan, J Jelita, W Simanjuntak, RTM Situmeang and PA Krisbiantoro. Highly efficient removal of Pb (II) and Cd (II) ions using magnesium hydroxide nanostructure prepared from seawater bittern by electrochemical method. *Colloid. Surf. Physicochem. Eng. Aspect* 2021; **631**, 127687.

[4] S Sharma, K Kumar, N Thakur, S Chauhan and M Chauhan. The effect of shape and size of ZnO nanoparticles on their antimicrobial and photocatalytic activities: A green approach. *Bull. Mater. Sci.* 2020; **43**, 20.

[5] H Amrulloh, A Fatiqin, W Simanjuntak, H Afriyani and A Annissa. Antioxidant and antibacterial activities of magnesium oxide nanoparticles prepared using aqueous extract of *Moringa oleifera* bark as green agents. *J. Multidiscip. Appl. Nat. Sci.* 2021; **1**, 44-53.

[6] YF He, DY Chu and Z Zhuo. Cycle stability of dual-phase lithium titanate (LTO)/TiO_2 nanowires as lithium battery anode. *J. Multidiscip. Appl. Nat. Sci.* 2021; **1**, 54-61.

[7] A Fadaka, O Aluko, S Awawu and K Theledi. Green synthesis of gold nanoparticles using Pimenta dioica leaves aqueous extract and their application as photocatalyst, antioxidant, and antibacterial agents. *J. Multidiscip. Appl. Nat. Sci.* 2021; **1**, 78-88.

[8] A Fatiqin, H Amrulloh, W Simanjuntak, I Apriani, RAHT Amelia, Syarifah, RN Sunarti and ARP Raharjeng. Characteristics of nano-size MgO prepared using aqueous extract of different parts of *Moringa oleifera* plant as green synthesis agents. *AIP Conf. Proc*. 2021; **2331**, 040001.

[9] H Amrulloh, A Fatiqin, W Simanjuntak, H Afriyani and A Annissa. Bioactivities of nano-scale magnesium oxide prepared using aqueous extract of *Moringa Oleifera* leaves as green agent. *Adv. Nat. Sci. Nanosci. Nanotechnol.* 2021; **12**, 015006.

[10] A Fatiqin, H Amrulloh and W Simanjuntak. Green synthesis of MgO nanoparticles using *Moringa oleifera* leaf aqueous extract for antibacterial activity. *Bull. Chem. Soc. Ethiopia* 2021; **35**, 161-70.

[11] H Amrulloh, W Simanjuntak, RTM Situmeang, SL Sagala, R Bramawanto, A Fatiqin, R Nahrowi and M Zuniati. Preparation of nano-magnesium oxide from Indonesia local seawater bittern using the electrochemical method. *Inorg. Nano-Metal Chem.* 2020; **50**, 693-8.

[12] HB Na, XF Zhang, M Zhang, ZP Deng, XL Cheng, LH Huo and S Gao. A fast response/recovery ppb-level H_2S gas sensor based on porous CuO/ZnO heterostructural tubule via confined effect of absorbent cotton. *Sensor. Actuator. B Chem.* 2019; **29**, 126816.

[13] J Singh, T Dutta, KH Kim, M Rawat, P Samddar and P Kumar. 'Green' synthesis of metals and their oxide nanoparticles: Applications for environmental remediation. *J. Nanobiotechnol*. 2018; **16**, 84.

[14] J Lillo-Ramiro, JM Guerrero-Villalba, MDL Mota-Gonz´alez, FS Aguirre-Tostado, G Guti´errez-Heredia, I Mejía-Silva and A Carrillo-Castillo. Optical and microstructural characteristics of CuO

thin films by sol gel process and introducing in non-enzymatic glucose biosensor applications. *Optik* 2021; **229**, 166238.
[15] R Nayak, FA Ali, DK Mishra, D Rayd, VK Aswald, SK Sahooe and B Nandaa. Fabrication of CuO nanoparticle: An efficient catalyst utilized for sensing and degradation of phenol. *J. Mater. Res. Tech.* 2020; **9**, 11045-59.
[16] ME Grigore, ER Biscu, AM Holban, MC Gestal and AM Grumezescu. Methods of synthesis, properties and biomedical applications of CuO nanoparticles. *Pharmaceuticals* 2016; **9**, 75.
[17] R Saemi, E Taghavi, H Jafarizadeh-Malmiri and N Anarjan. Fabrication of green ZnO nanoparticles using walnut leaf extract to develop an antibacterial film based on polyethylene-starch-ZnO NPs. *Green Process. Synth.* 2021; **10**, 112-4.
[18] S Alamdari, MS Ghamsari, C Lee, W Han, HH Park, MJ Tafreshi, H Afarideh and MHM Ara. Preparation and characterization of zinc oxide nanoparticles using leaf extract of *Sambucus ebulus*. *Appl. Sci.* 2020; **10**, 3620.
[19] AAM Sakib, SM Masum, J Hoinkis, R Islam and MAI Molla. Synthesis of CuO/ZnO nanocomposites and their application in photodegradation of toxic textile dye. *J. Compos. Sci.* 2019; **3**, 91.
[20] A Marcu and C Viespe. Laser-grown ZnO nanowires for room-temperature SAW-sensor applications. *Sensor. Actuator. B* 2015; **208**, 1-6.
[21] GA Govindasamy, RBSMN Mydin, S Sreekantan and NH Harun. Compositions and antimicrobial properties of binary ZnO-CuO nanocomposites encapsulated calcium and carbon from *Calotropis gigantea* targeted for skin pathogens. *Sci. Rep*. 2021; **11**, 99.
[22] A Anu and MA Khadar. CuO-ZnO nanocomposite films with efficient interfacial charge transfer characteristics for optoelectronic applications. *SN Appl. Sci.* 2019; **1**, 1057.
[23] SA Hassanzadeh-Tabrizi, MM Motlagh and S Salahshour. Synthesis of ZnO/CuO nanocomposite immobilized on γ-Al_2O_3 and application for removal of methyl orange. *Appl. Surf. Sci.* 2016; **384**, 237-43.
[24] N Abraham, RR Krishnakumar, C Unni and D Philip. Simulation studies on the responses of ZnO-CuO/CNT nanocomposite based SAW sensor to various volatile organic chemicals. *J. Sci. Adv. Mater. Dev.* 2019; **4**, 125-31.
[25] S Das and VC Srivastava. Synthesis and characterization of ZnO/CuO nanocomposite by electrochemical method. *Mater. Sci. Semicond. Process.* 2017; **57**, 173-7.
[26] SM Mali, SS Narwade, YH Navale, SB Tayade, RV Digraskar, VB Patil, AS Kumbhar and BR Sathe. Heterostructural CuO-ZnO nanocomposites: A highly selective chemical and electrochemical NO_2 sensor. *ACS Omega* 2019; **4**, 20129-41.
[27] NLU Vo, TTV Nguyen, T Nguyen, PA Nguyen, VM Nguyen, NH Nguyen, VL Tran, NA Phan and KPH Huynh. Antibacterial shoe insole-coated CuO-ZnO nanocomposite synthesized by the sol-gel technique. *J. Nanomater*. 2020; **2020**, 8825567.
[28] J Sandhya and S Kalaiselvam. UV responsive quercetin derived and functionalized CuO/ZnO nanocomposite in ameliorating photocatalytic degradation of rhodamine B dye and enhanced biocidal activity against selected pathogenic strains. *J. Environ. Sci. Health A* 2021; **56**, 835-48.
[29] CP Sagita, L Nulandaya and YS Kurniawan. Efficient and low-cost removal of methylene blue using activated natural kaolinite material. *J. Multidiscip. Appl. Nat. Sci.* 2021; **1**, 69-79.
[30] TT Li, N Bao, A Geng, H Yu, Y Yang and XT Dong. Study on room temperature gas-sensing performance of CuO film-decorated ordered porous ZnO composite by In_2O_3 sensitization. *R. Soc. Open Sci.* 2018; **5**, 171788.
[31] S Soltani, U Rashid, IA Nehdi and SI Al-Resayes. Esterification of palm fatty acid distillate using a sulfonated mesoporous CuO-ZnO mixed metal oxide catalyst. *Chem. Eng. Tech.* 2017; **40**, 1931-9.
[32] MA Khan, Y Wahab, R Muhammad, M Tahir and S Sakrani. Catalyst-free fabrication of novel ZnO/CuO core-Shell nanowires heterojunction: Controlled growth, structural and optoelectronic properties. *Appl. Surf. Sci.* 2018; **435**, 718-32.
[33] D Manyasree, KM Peddi and R Ravikumar. CuO nanoparticles: Synthesis, characterization and their bactericidal efficacy. *Int. J. Appl. Pharmaceut.* 2017; **9**, 71-4.
[34] R Kumar, O Al-Dossary, G Kumar and A Umar. Zinc oxide nanostructures for NO_2 gas-sensor applications: A review. *Nano-Micro Lett.* 2015; **7**, 97-120.
[35] S Das and VC Srivastava. An overview of the synthesis of CuO-ZnO nanocomposite for environmental and other applications. *Nanotechnol. Rev.* 2018; **7**, 267-82.

[36] B Fatima, SI Siddiqui, R Ahmad, NTT Linh and VN Thai. CuO-ZnO-$CdWO_4$: A sustainable and environmentally benign photocatalytic system for water cleansing. *Environ. Sci. Pollut. Res.* 2021; **28**, 53793-803.

[37] W Fang, L Yu and L Xu. Preparation, characterization and photocatalytic performance of heterostructured CuO-ZnO-loaded composite nanofiber membranes. *Beilstein J. Nanotechnol.* 2020; **11**, 631-50.

[38] D Saravanakkumar, HA Oualid, Y Brahmi, A Ayeshamariam, M Karunanaithy, AM Saleem, K Kaviyarasu, S Sivaranjani and M Jayachandran. Synthesis and characterization of CuO/ZnO/CNTs thin films on copper substrate and its photocatalytic applications. *OpenNano* 2019; **4**, 100025.

[39] G Zhou, L Long, P Wang, Y Hu, Q Zhang, C Liu. Designing CuO/ZnO nanoforest device toward optimal photocatalytic performance through structure and facet engineering. *Mater. Lett.* 2020; **273**, 127907.

[40] A Sankaran and K Kumaraguru. The novel two step synthesis of CuO/ZnO and CuO/CdO nanocatalysts for enhancement of catalytic activity. *J. Mol. Struct.* 2020; **1221**, 128772.

[41] MS AlSalhi, A Sakthisabarimoorthi, S Devanesan, SAMB Dhas and M Jose. Study on photocatalytic and impedance spectroscopy investigations of composite CuO/ZnO nanoparticles. *J. Mater. Sci. Mater. Electron.* 2019; **30**, 13708-18.

[42] H Salari and M Sadeghinia. MOF-templated synthesis of nano Ag_2O/ZnO/CuO heterostructure for photocatalysis. *J. Photochem. Photobiol. A Chem.* 2019; **376**, 279-87.

[43] P Sathishkumar, R Sweena, JJ Wu and S Anandan. Synthesis of CuO-ZnO nanophotocatalyst for visible light assisted degradation of a textile dye in aqueous solution. *Chem. Eng. J.* 2011; **171**, 136-40.

[44] M Naseer, U Aslam, B Khalid and B Chen. Green route to synthesize zinc oxide nanoparticles using leaf extracts of *Cassia fistula* and *Melia azadarach* and their antibacterial potential. *Sci. Rep.* 2020; **10**, 9055.